tvst

Article

Intrastromal Injection of Hyaluronidase Alters the Structural and Biomechanical Properties of the Corneal Stroma

Soohyun Kim[1,*], Iman Jalilian[1,*], Sara M. Thomasy[1,2,†], Morgan A. W. Bowman[1], Vijay Krishna Raghunathan[3,4], Yeonju Song[1], Cynthia A. Reinhart-King[5], and Christopher J. Murphy[1,2,†]

[1] Department of Surgical and Radiological Sciences, School of Veterinary Medicine, University of California Davis, Davis, CA, USA
[2] Department of Ophthalmology & Vision Science, School of Medicine, University of California Davis, Davis, CA, USA
[3] Department of Basic Science, College of Optometry, University of Houston, Houston, TX, USA
[4] Department of Biomedical Engineering, Cullen College of Engineering, University of Houston, Houston, TX, USA
[5] Department of Biomedical Engineering, School of Engineering, Vanderbilt University, Nashville, TN, USA

Correspondence: Christopher J. Murphy, University of California-Davis, 1 Shields Avenue, Davis, CA 95616, USA. e-mail: cjmurphy@ucdavis.edu
Sara M. Thomasy, University of California-Davis, 1 Shields Avenue, Davis, CA 95616, USA. e-mail: smthomasy@ucdavis.edu

Received: October 18, 2019
Accepted: January 5, 2020
Published: May 21, 2020

Keywords: cornea; stroma; hyaluronidase; glycosaminoglycans; atomic force microscopy

Citation: Kim S, Jalilian I, Thomasy SM, Bowman MAW, Raghunathan VK, Song Y, Reinhart-King CA, Murphy CJ. Intrastromal injection of hyaluronidase alters the structural and biomechanical properties of the corneal stroma. Trans Vis Sci Tech. 2020;9(6):21, https://doi.org/10.1167/tvst.9.6.21

Purpose: Glycosaminoglycans (GAGs) are important components of the corneal stroma, and their spatiotemporal arrangement regulates the organization of collagen fibrils and maintains corneal transparency. This study was undertaken to determine the consequences of hyaluronidase (HAse) injected into the corneal stroma on stromal stiffness and ultrastructure.

Methods: Equal volumes of HAse or balanced salt solution (vehicle) were injected intrastromally into the corneas of New Zealand white rabbits. Ophthalmic examination and multimodal imaging techniques, including Fourier-domain optical coherence tomography and in vivo confocal microscopy (IVCM), were performed at multiple time points to evaluate the impact of HAse treatment in vivo. Atomic force microscopy and transmission electron microscopy (TEM) were used to measure corneal stiffness and collagen's interfibrillar spacing, respectively.

Results: Central corneal thickness progressively decreased after HAse injection, reaching its lowest value at day 7, and then returned to normal by day 42. The HAse did not impact the corneal endothelium but transiently altered keratocyte morphology at days 1 and 7, as measured by IVCM. HAse-injected corneas became stiffer by day 1 postinjection, were stiffest at day 7, and returned to preinjection values by day 90. Changes in stromal stiffness correlated with decreased interfibrillar spacing as measured by TEM.

Conclusions: Degradation of GAGs by HAse decreases the corneal thickness and increases stromal stiffness through increased packing of the collagen fibrils in a time-dependent manner.

Translational Relevance: Intrastromal HAse injection appears relatively safe in the normal cornea, but its impact on corneal biomechanics and structure under pathologic conditions requires further study.

Introduction

Transparency of the cornea is maintained through regular packing of collagen fibrils within a proteoglycan- and glycosaminoglycan (GAG)–rich matrix.[1] In particular, GAGs such as keratan sulfate (KS), chondroitin sulfate (CS), and hyaluronic acid (HA)[2–4] are critical for the maintenance of the extremely ordered interfibrillar spacing of the corneal stroma.[5–7] While it is accepted that the negatively charged GAGs help withstand compressive forces and contribute to viscoelastic behavior, there remains a significant knowledge gap in regard to the influence of GAGs on the biomechanical properties of the corneal stroma in health or disease. Physical insults such as wounding markedly alter the mechanical properties, structures, and transparency of the stroma.[8]

A bidirectional relationship between keratocytes, the native cells of the stroma, and their extracellular matrix (ECM) is present whereby the keratocytes produce and remodel the ECM that surrounds them, with changes in the structure and biomechanics of the ECM profoundly influencing the behavior of the stromal cells.[9–12]

Mammalian hyaluronidase (HAse) has hydrolytic and transglycosidase activity and can digest a variety of GAGs of the ECM, including HA, CS, and KS.[13] Consequently, HAse can alter tissue ultrastructure[14] and has been extensively used as a spreading agent to facilitate the infusion of injected drugs into the skin and the eye.[15,16] Specifically, HAse has been used to enhance the penetration of local anesthetics in ophthalmic surgery[16] and has been reported to accelerate cutaneous wound healing in mice.[17] Proposed uses of HAse also include induction of vitreous liquefaction,[18,19] increasing aqueous outflow as a treatment for glaucoma,[20,21] and preventing elevation of intraocular pressure associated with HA-containing viscoelastic materials.[22] Given that the cornea is rich in GAGs, HAse has been suggested as a therapy to decrease corneal scarring[23] or soften the corneal stroma possibly through altering its structure.[14] The enzymatic effect of HAse has also been investigated ex vivo in combination with surgical procedures such as deep anterior lamellar keratoplasty (DALK).[24,25] These studies showed that HAse facilitated the separation of corneal stroma from Descemet's membrane (DM) in patients, possibly through cleavage of chemical bonds between the stromal lamellae and/or between lamellae and DM. Despite its widespread medical use, little is known about the effects of HAse on the mechanical and ultrastructural properties of tissues, including the cornea. In this study, we took advantage of the highly organized structure of the cornea to quantitatively characterize the enzymatic effects of HAse on the biomechanical properties and collagen fibril spacing of its stroma in vivo.

Materials and Methods

Cell Isolation, Culture, and Viability Test

Primary keratocytes were isolated from freshly enucleated young rabbit eyes (Pel-Freez Biologicals, Rogers, AR) as previously described.[9] Cells were cultured in low-glucose Dulbecco's modified Eagle's medium (Gibco BRL, Grand Island, NJ) supplemented with 10% fetal bovine serum and 1% Pen/Strep/Fungizone (HyClone 100X; HyClone, Logan, UT) and incubated for 3 days to ensure transition to the fibroblast phenotype. All assays were conducted between passages 3 and 5. Effects of HAse on the viability of rabbit corneal fibroblasts (RCFs) were evaluated using the 3-[4,5-dimethylthiazol-2-yl]-2,5 diphenyl tetrazolium bromide (MTT) assay. RCFs were plated into 96-well plates at a density of 2×10^3 cells per well in 100 µL culture medium and allowed to attach for 24 hours before treatment. Then, HAse at concentrations ranging from 0.0002 to 2000 U/mL or an equal amount of phosphate-buffered saline (PBS) (vehicle control) were used; 0.1% saponin was used as a positive control. Cells were treated for 24, 48, and 72 hours. Then, the MTT (0.5 mg/mL) solution was added to each well and incubated for 4 hours at 37°C. Next, the culture medium supernatant was carefully aspirated from the wells without disturbing the formazan precipitate. The formazan crystals were dissolved in 50 µL/well dimethyl sulfoxide (Sigma Chemical Co., St. Louis, MO) and mixed thoroughly, and then the absorbance was measured at 540 nm using a microplate spectrophotometer. Results were expressed as relative percentage viability compared with the vehicle control. Experiments were performed in triplicate.

Determination of HAse Activity

The HAse activity in culture medium was analyzed at 24, 48, and 72 hours using a hyaluronidase activity enzyme-linked immunosorbent assay (ELISA) kit (K-6000; Echelon Biosciences, Inc., Salt Lake City, UT) following the manufacturer's protocol. Each experiment was performed in triplicate. This assay was also used for measurements of HAse activity in aqueous humor at days 1, 7, and 90 after the HAse or balanced salt solution (BSS; Alcon, Fort Worth, TX) intrastromal injection into the in vivo rabbit cornea. To measure the HAse activity of the aqueous humor, 50 µL aqueous humor was collected immediately after euthanasia and HAse activity was measured.

Effects of HAse Injection in the Ex Vivo Rabbit Cornea

A total of 9 commercially purchased (Pel-Freez Biologicals) rabbit eyes were used within 6 hours of euthanasia. To determine the distribution of fluid following intrastromal injection, 100 µL 4′-6-diamidino-2-phenylindole (DAPI; Life Technologies, Carlsbad, CA) diluted in BSS (1:5000) was injected intrastromally at superior, inferior, nasal, and temporal sites adjacent to the limbus (25 µL/site) using 6 ex vivo eyes. Corneal buttons from 3 eyes were excised

and fixed immediately after the injection. The remaining 3 eyes were incubated at 37°C for 24 hours, and then the corneal buttons were fixed with 10% formalin. Fixed corneal buttons were processed using standard protocols and embedded in paraffin wax. Then, 5-µm-thick parasagittal sections were obtained from paraffin blocks, paraffins were removed using xylene (10-minute incubation for 2 cycles), and samples were rehydrated using serial dilutions of ethanol. The sections were imaged using an Axiovert 200M epifluorescent microscope (Carl Zeiss Ag, Oberkochen, Germany) and a 10× objective.

The effect of HAse on corneal stromal stiffness was determined ex vivo prior to initiating in vivo experiments. Immediately following euthanasia, the left globes from 9 rabbits (normal, n = 3; BSS injection, n = 3; and HAse injection, n = 3) were used to determine the effect of HAse injection on elastic modulus by atomic force microscopy (AFM). HAse (1000 U/100 µL) or an identical volume of BSS was injected intrastromally using the same procedure to the aforementioned DAPI injection. The ex vivo eyes were incubated at 37°C for 24 hours and elastic modulus was measured by AFM as detailed below.

Animals

A total of 16 New Zealand White female rabbits (Charles River laboratories, Wilmington, MA) with a mean age of 2 ± 0.0 months and body weight of 3.6 ± 0.2 kg were utilized in this study and assigned to the following groups: no injection (n = 3) and postinjection day 1 (n = 4), day 7 (n = 6), and day 90 (n = 3). The study design was approved by the Institutional Animal Care and Use Committee of the University of California, Davis and performed in compliance with the Association of Research in Vision and Ophthalmology statement for the use of animals in ophthalmic and vision research. A complete ophthalmic examination and advanced ocular imaging studies were performed prior to inclusion into the study; only animals free of ocular disease were used.

Intrastromal Injection and Postinjection Treatment

Rabbits were premedicated with midazolam (0.7 mg/kg, intramuscular injection [IM]) and hydromorphone (0.1 mg/kg, IM) followed by ketamine (10–30 mg/kg, IM) for induction and maintenance of anesthesia. Then, 1000 U HAse or BSS at a total volume of 100 µL was injected intrastromally at 4 different sites (25 µL/site; superior, inferior, nasal, and temporal cornea) using 0.5-mL insulin syringes attached to 30-gauge, half-inch needles (BD Micro-Fine; BD, Franklin Lakes, NJ). The needle was inserted into stroma parallel to the corneal surface at the limbus at each site, and 25 µL solution was injected to form ~4-mm bleb at each site. Ofloxacin 0.3% ophthalmic solution (Alcon, Hunenberg, Switzerland) was administered once OU (oculus uterque, both eyes) following the intrastromal injection; buprenorphine (0.03–0.06 mg/kg, IM) was administered to reverse the hydromorphone and to provide analgesia.

Clinical Evaluation and Advanced Imaging

A complete ophthalmic examination and advanced imaging were performed prior to and at days 0, 1, 3, 7, 14, 21, 28, 42, 56, and 90 following injection. The semiquantitative preclinical ocular toxicology scoring[26] was used in this study to assess the anterior and posterior segment using a handheld slit-lamp biomicroscope (SL-15; Kowa Optimed, Torrance, CA) and an indirect ophthalmoscope (Keeler VANTAGE Plus; Keeler Inc., Broomall, PA) with a 28-D indirect lens (Volk Optical, Inc., Mentor, OH); ocular findings were documented with a digital color camera (Canon EOS5D; flash 1/32, ISO 200, F16, Canon Inc., Tokyo, Japan). Rebound tonometry was performed to measure intraocular pressure (TonoVet; Icare, Helsinki, Finland), and ultrasonic pachymetry (USP; Accupach VI; Accutome, Malvern, PA) was performed to assess corneal thickness by placing the probe perpendicular to the cornea after applying a drop of 0.5% proparacaine (Alcon, Inc., Fort Worth, TX). Fluorescein stain was applied to assess epithelial integrity and imaged with digital photography (Nikon D300; flash 1/4, ISO 250, F11, Nikon Inc., Tokyo, Japan) with cobalt blue filters (Blue-AWB; Nikon) over the flash and a yellow filter (HOYA HMC 62 mm Y [K2], Kenko Tokina Co., Ltd, Tokyo, Japan) covering the lens. Fourier-domain optical coherence tomography (FD-OCT; RTVue 100, software version 6.1; Optovue Inc., Fremont, CA) with CAM-L (S/N 40107; 8-mm scan length) or CAM-S (S/N 30107; 3-mm scan length) lenses was used to assess the morphology of the central cornea in vivo. To evaluate keratocytes and corneal endothelial cells in live rabbits, in vivo confocal microscopy (IVCM) (Heidelberg Retinal Tomography 3 in conjunction with the Rostock Cornea Module; Heidelberg Engineering, Dossenheim, Germany) was performed. Serial scans of IVCM were collected with 100 images/scan, and stromal images 50 to 60 µm apart from basal cell layer and endothelium were used to identify keratocytes in the anterior and posterior stroma, respectively. Manual counts of keratocyte and endothelial cell

density were performed using the Heidelberg Eye Explorer (software version 1.7.0; Heidelberg Engineering). Three images per eye were analyzed and the average was taken. For cell counts, cells touching the borders were counted only along one top or bottom border and one right or left border. Cells touching the opposite two borders were omitted from analysis.

Tissue Harvest and Processing

Rabbits were euthanized with pentobarbital (200 mg/kg, intravenous). After marking the central corneal area with an 8-mm trephine, half of the corneal epithelium was mechanically debrided and the basement membrane and anterior stroma were ablated with an excimer laser (NIDEK EC5000; Nidek Technologies, Gamagori, Japan), 6 mm in diameter and 100 µm in depth, with half of the ablation zone covered with an EC-5000 calibration card (Nidek Technologies) to constrain laser ablation to a semicircular geometry. An 8-mm central corneal button was then harvested using a biopsy punch and corneal scissors. The corneal buttons were sectioned into 4 pieces using a razor blade. The sections ablated with the laser were submitted for AFM, while the remaining 2 corneal sections with intact epithelium were fixed in 10% neutral buffered formalin or 2.5% glutaraldehyde and 2% paraformaldehyde in 0.1 M sodium cacodylate buffer for light and transmission electron microscopy, respectively.

Atomic Force Microscopy

To measure the elastic modulus of the corneal stroma, AFM was used as previously described.[27] Briefly, force versus indentation curves were obtained using the MFP-3D Bio AFM (Asylum Research, Santa Barbara, CA) mounted on a Zeiss Axio Observer inverted microscope (Carl Zeiss, Thornwood, NY). To functionalize the cantilever, a dry borosilicate glass bead with a nominal radius of 4.6 to 5.9 µm (Thermo Scientific, Fremont, CA) was glued to the end of a silicon nitride PNP-TR-50 cantilever with actual spring constant (κ) of 55 to 246 pN nm^{-1} and length of 100 µm (Nano World, Switzerland, Neuchatel, Switzerland). Deflection sensitivity of the probes was measured by taking the average of 5 force curves on a glass slide in Dulbecco's phosphate-buffered saline. The spring constant of each cantilever probe used for the indentation measurements was determined using a thermal tuning method. To measure the stiffness of the rabbit corneas, corneal sections were adhered to the AFM dishes using cyanoacrylate glue. All samples were equilibrated in Hank's balanced salt solution (HBSS) for at least 60 minutes prior to obtaining measurements to minimize thermal drift. For all samples, 5 force curves at 2 µm s^{-1} were obtained from 5 to 10 random positions. Elastic modulus (E) of each sample was obtained by fitting the indentation force versus the indentation depth of the sample and further by applying the Hertz model for a spherical tip, as shown in equation (1),

$$F = (4/3) * (E/(1 - \nu^2)) * \delta^{3/2} * R^{1/2}, \qquad (1)$$

where F is the force applied by the indenter, E is Young's modulus, ν is Poisson's ratio (assumed to be 0.5 for biological samples), δ is the indentation depth, and R is the radius of the tip.

Histopathology and Transmission Electron Microscopy

The formalin-fixed corneal sections were embedded in paraffin, sectioned 5 µm thick at the parasagittal plane, and stained with hematoxylin and eosin (H&E; Fisher Scientific, St. Louis, MO) prior to evaluation with light microscopy. The corneal sections fixed in 2.5% glutaraldehyde and 2% paraformaldehyde in 0.1 M sodium cacodylate buffer were used to examine by transmission electron microscopy (TEM) using standard protocols. Briefly, the fixed corneal buttons were rinsed in 0.1 M sodium cacodylate buffer for 15 minutes twice and then placed in 2% osmium tetroxide for 1 hour. The samples were then rinsed in water twice, 15 minutes each time. Next, samples were serially dehydrated in 50% ethyl alcohol (EtOH), 75% EtOH, and 95% EtOH for 30 minutes and then twice with 100% EtOH, 20 minutes each time (40 minutes total). Samples then were placed in propylene oxide for another 30 minutes. Finally, the corneal buttons were infiltrated in a Poly/Bed 812 mixture for 4 hours and polymerized in a Poly/Bed 812 mixture at 65°C for at least 24 hours. Ultrathin sections were mounted on naked copper grids and stained with 3% uranyl acetate and 0.03% lead citrate before examination with TEM (Philips CM120 Biotwin Lens, F.E.I. Company, Hillsboro, OR; with GatanMegaScan, model 794/20, digital camera [2K × 2K], Pleasanton, CA; Gatan BioScan, model 792, Pleasanton, CA).

Analysis of TEM Micrographs

Interfibrillar spacing in the anterior and posterior stroma was measured using MATLAB software (The MathWorks, Inc., Natick, MA). Ten different locations per image (6 images in total) at both anterior and posterior aspects of the stromal samples were analyzed for each sample. A collagen fibril was selected as the central

point, defined as a core fibril. Then 6 adjacent fibrils surrounding the core fibril defining a hexagon were selected. The center of all fibrils was marked, and then the interfibrillar distance between the core fibril and the surrounding fibrils was measured in MATLAB. ImageJ (version 1.51j8; National Institutes of Health, Bethesda, MD) was used to measure the diameter of collagen fibrils.

Statistical Analysis

Data were presented as mean ± SD and statistical analysis was performed with GraphPad Prism 7.03 (GraphPad Software, Inc., San Diego, CA). All data sets were compared with 1-way analysis of variance (ANOVA) or 2-way ANOVA as indicated. When variability between the data set means was determined to be significant, Tukey's multiple comparisons test was used to compare these date sets. Values of $P < 0.05$ were considered statistically significant.

Results

Effect of HAse on Cell Viability and Its Enzymatic Activity

The toxicity of HAse was tested on RCFs at different time points (24, 48, and 72 hours) using an in vitro viability assay (Supplementary Fig. S1A). At lower concentrations (0.0002–0.02 U/mL), HAse showed no toxicity for RCFs, and cell viability was comparable between PBS-treated (control) and HAse-treated cells. However, a gradual decrease in viability of RCFs was observed at higher concentrations of HAse (0.2–2000 U/mL) at all incubation time points compared with controls. The reduction in cell viability attributable to HAse was markedly less than that of the positive control, 0.1% saponin (Supplementary Fig. S1A). A gradual but significant decrease in HAse activity, as measured by ELISA, was observed 24, 48, and 72 hours after incubation compared with the initiation of the experiment (Supplementary Fig. S1B, $P < 0.001$).

Following the in vitro experiments, the enzymatic activity of HAse was measured in vivo (Fig. 1). A marked increase in HAse activity was observed in aqueous humor 1 day following the HAse injection (53.0% ± 7.2%, $P < 0.001$) in comparison to BSS and untreated controls (26.9% ± 0.6% and 23.1% ± 0.5%, respectively). At 7 days postinjection, HAse activity in aqueous humor had decreased (36.9% ± 2.1%, $P = 0.02$), although the measured values were still significantly higher than BSS and untreated controls (25.7% ± 1.1% and 23.1% ± 0.5%, respectively). At day 90, HAse activity in aqueous humor of the HAse-injected eyes did not significantly differ from the BSS or untreated controls (18.9% ± 2.3% vs. 20.5% ± 1.5%, $P > 0.99$).

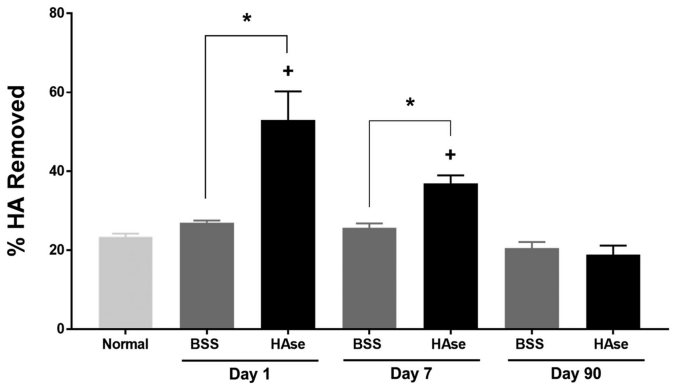

Figure 1. HAse enzymatic activity in cornea decreases over time. Following intrastromal injection of 1000 U HAse to 16 rabbits, HAse activity in aqueous humor, as measured by ELISA, was greatest at day 1 and then declined by day 7 but was still significantly greater than BSS or untreated controls. By day 90, no HAse activity was observed in HAse-injected corneas, which was comparable to BSS and untreated controls. Results are expressed as mean ± SD. $^{+}P < 0.05$ compared with the untreated cornea, $^{*}P < 0.05$ between the HAse- and BSS-treated groups at the same time point, 1-way ANOVA, followed by Tukey's pairwise multiple comparison test.

Ophthalmic Examination and the Central Corneal Thickness

To determine the distribution of intrastromal injections in the rabbit cornea, a mixture of BSS and DAPI was injected into the stroma and its diffusion rate was monitored ex vivo. The BSS-DAPI mixture was evenly distributed throughout the cornea, from the limbus to central cornea 24 hours after the injection (Supplementary Fig. S1C).

Transient corneal edema was observed in both HAse- and BSS-injected eyes at day 1 postinjection, but the cornea remained transparent throughout the remainder of the study (Fig. 2A). Conjunctival hyperemia was observed at the superior perilimbal region from days 1 to 7 in HAse- and BSS-injected eyes. In addition, transient and mild corneal neovascularization, shorter than 2 mm in length, was observed in HAse-injected corneas at the superior perilimbal cornea on days 14, 21, and 28 (Supplementary Fig. S2). Intraocular pressure remained within normal published ranges (13 ± 6 mm Hg)[28] in all eyes at all time points throughout the study. However, the HAse-injected eyes showed a significant decrease of intraocular pressure (IOP) at day 3 (10.6 ± 2.5 mm Hg) after

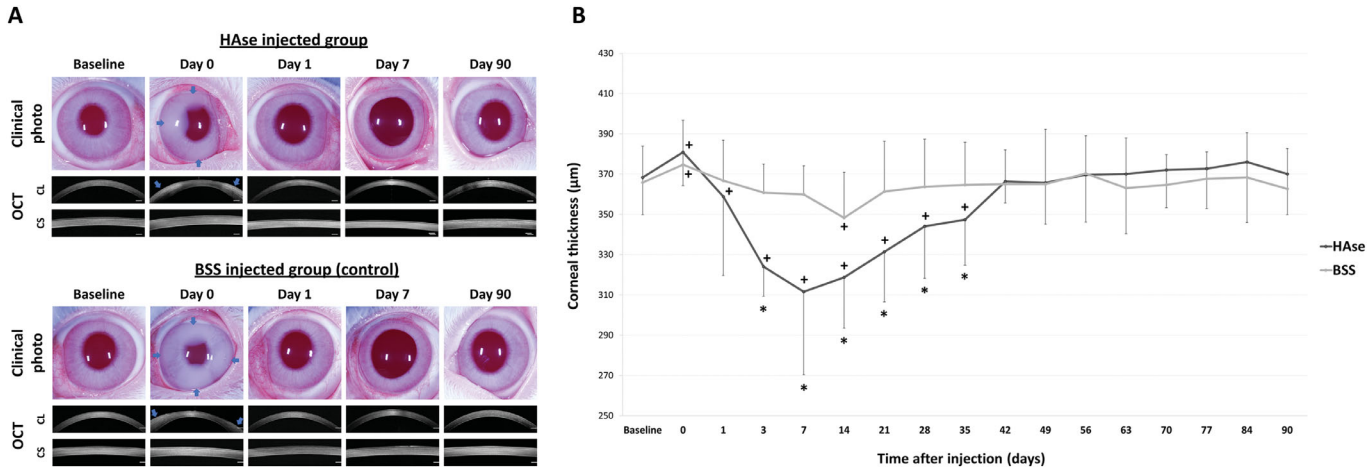

Figure 2. Intrastromal injection of HAse did not impact corneal transparency but decreased CCT. (A) In total, 1000 U/eye of HAse was injected intrastromally (4 sites at 25 µL/site; *blue arrows*) to the right eye of 12 rabbits and an equal volume of BSS (vehicle) was injected in the left eye as a control; corneal edema was observed in the peripheral cornea postinjection in both groups. However, HAse-injected areas (*blue arrows*) returned to normal transparency on day 1 following injection. The FD-OCT images demonstrated increased thickness and echogenicity immediately following injection of HAse or BSS in the peripheral stroma using a corneal long-lens module (CL) with an 8-mm scan length. At days 1 and 7 postinjection, CCT was significantly thinner in HAse- versus BSS-injected corneas as demonstrated with FD-OCT using a short-lens module (CS) with a 3-mm scan length in the central cornea. (B) Using ultrasonic pachymetry, maximal reduction in CCT was observed at 7 days postinjection and then returned to baseline (+) at day 35 in HAse- versus BSS-treated eyes (*). Results are expressed as mean ± SD. $^{+}P < 0.05$ compared to baseline, $^{*}P < 0.05$ between the groups at the same time point; 1-way ANOVA, followed by Tukey's pairwise multiple comparison test.

the intrastromal injection compared to baseline (15.2 ± 2.9 mm Hg, $P = 0.005$) (Supplementary Fig. S3).

FD-OCT images demonstrated normal corneal morphology in both HAse- and BSS-injected eyes throughout the study other than a transient increase in thickness and reflectivity on day 0 immediately after the injection (Fig. 2B). At baseline, mean central corneal thickness (CCT) for HAse-injected eyes did not significantly differ from BSS-injected eyes at 368 ± 19 and 366 ± 18 µm, respectively ($P > 0.99$, Fig. 2B). Immediately following injection, mean CCT significantly increased for both treatment groups ($P = 0.04$). At 3 days postinjection, HAse-injected corneas were significantly thinner than BSS-injected corneas (324 ± 15 µm vs. 361 ± 14 µm, $P < 0.001$) with CCT thinnest at 7 days after HAse-injection (312 ± 13 µm, $P < 0.001$). CCT then gradually returned to normal at 42 days following the HAse injection.

Morphology of the Keratocytes and Corneal Endothelium by IVCM

At days 1 and 7 post-HAse injection, a transient change in the morphology of the keratocytes was observed by IVCM. Keratocytes were thinner and more elongated compared with noninjected and BSS-injected controls (Fig. 3A). However, keratocyte morphology returned to normal by day 90 postinjection of HAse (Fig. 3A). Anterior stromal keratocyte density was significantly decreased in the HAse- and BSS-injected groups at day 1 versus baseline ($P = 0.004$ and 0.04, respectively) (Fig. 3B). Posterior stromal keratocyte density did not significantly differ by group ($P = 0.51$) or over time ($P = 0.47$). Endothelial cell morphology remained unchanged in all 3 groups with a density >2500 cells/mm^2 maintained throughout the study (Fig. 3A, 3B); no significant differences were observed between groups ($P = 0.47$) or over time ($P = 0.68$).

Elastic Modulus of the Corneal Stroma

The influence of HAse on the stromal stiffness was first measured ex vivo using AFM. The AFM force curve analysis documented a significant increase in the stiffness of HAse-injected corneas versus BSS and untreated controls at 24 hours after injection at 2.28 ± 2.11, 1.42 ± 1.12, and 1.61 ± 1.07 kPa, respectively ($P < 0.001$) (Supplementary Fig. S1D).

Then, the elastic modulus of the HAse-injected corneas was compared with BSS-injected and normal, uninjected corneas in vivo (Fig. 4). At day 1 postinjection, the stiffness of HAse-injected corneas was significantly increased versus normal corneas (2.18 ± 0.47 vs. 1.28 ± 0.10 kPa, $P = 0.03$) but not versus BSS-treated corneas (1.45 ± 0.19 kPa, $P = 0.12$) (Fig. 4). At day 7, the stiffness of HAse-injected corneas (2.63

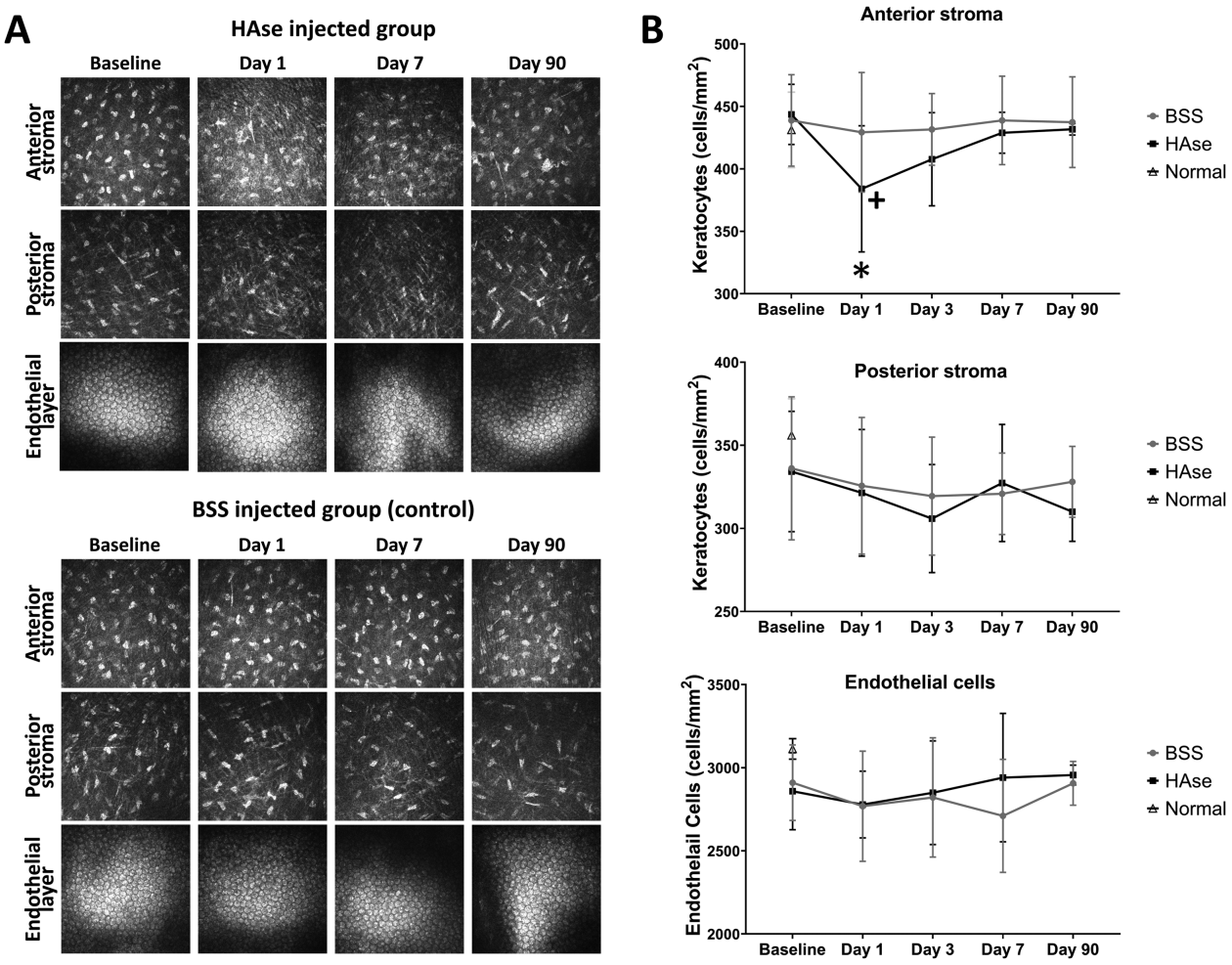

Figure 3. Intrastromal injection of HAse transiently altered keratocytes but not endothelial morphology imaged by IVCM. (A) Keratocytes were more elongated and polarized at days 1 and 7 in HAse-injected corneas compared to BSS controls. These morphologic alterations were more severe in the anterior versus posterior stroma. Endothelial cell morphology and density were not affected at any time point in any of the 3 groups. (B) Anterior stromal keratocyte density in the HAse- and BSS-injected groups was significantly reduced at day 1 compared with baseline ($P = 0.004$ and 0.04, respectively). Posterior stromal keratocyte and endothelial cell densities did not differ by group or time. Results are expressed as mean ± SD. $^{+}P < 0.05$ compared to baseline in same group, $^{*}P < 0.05$ between the groups at the same time point; 2-way ANOVA, followed by Tukey's multiple comparison test.

± 0.53 kPa) was significantly greater than both BSS (1.73 ± 0.37 kPa, $P = 0.015$) and untreated controls (1.28 ± 0.10 kPa, $P < 0.001$) (Fig. 4). At day 90, the elastic modulus of the HAse-injected corneas had returned to normal (1.22 ± 0.44 kPa) and did not significantly differ from BSS (1.42 ± 0.06 kPa, $P = 0.99$) or untreated controls (1.28 ± 0.10 kPa, $P > 0.99$) (Fig. 4).

Light and Transmission Electron Microscopy: Interfibrillar Spacing of Stromal Collagen Fibers

For all time points and groups, evaluation of H&E-stained sections were unremarkable. TEM was used to assess the effect of HAse on corneal stromal structure and also interfibrillar spacing (Fig. 5A). We utilized an in-house developed MATLAB program to quantitatively measure the distances between the collagen fibrils in both HAse- and BSS-injected corneas at all time points (Fig. 5B). A significant reduction in collagen interfibrillar spacing was observed 1 day after the HAse injection (49.9 ± 3.4 and 48.1± 3.5 nm for anterior and posterior stroma, respectively, $P = 0.006$ and $P = 0.05$) when compared with the BSS (54.8 ± 1.6 and 53.4 ± 4.7 nm for anterior and posterior stroma, respectively) and untreated controls (52.8 ± 2.2 and 50.7 ± 3.1 nm for anterior and posterior stroma, respectively). The greatest reduction in interfibrillar spacing was observed 7 days post-HAse injection (45.5 ± 2.3 and 41.9 ± 3.6 nm for anterior and posterior stroma,

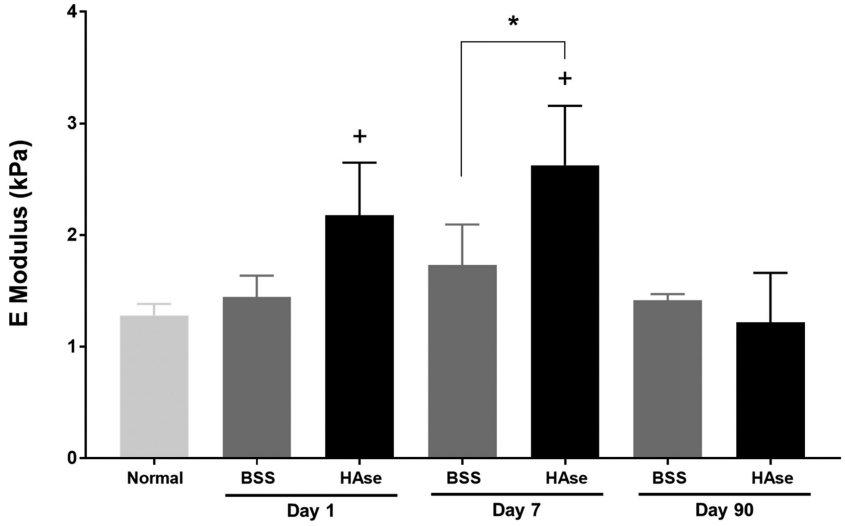

Figure 4. The intrastromal injection of HAse significantly but transiently increased corneal stiffness. At day 1, HAse-injected corneas showed a significantly greater elastic modulus versus untreated corneas. By day 7, elastic modulus was maximal and significantly greater in HAse-injected corneas versus BSS-treated and untreated controls. By day 90, elastic modulus of the HAse-injected corneas had returned to baseline and did not differ from the 2 groups. Results are expressed as mean ± SD. $^{+}P < 0.05$ compared to baseline, $^{*}P < 0.05$ between the HAse- and BSS-treated groups at the same time point, n = 4 per group, 1-way ANOVA, followed by Tukey's pairwise multiple comparison test.

respectively, $P < 0.001$ at both locations) versus BSS controls (52.4 ± 2.8 and 54.9 ± 3.1 nm for anterior and posterior stroma, respectively). At 90 days post-HAse injection, collagen interfibrillar spacing had normalized (53.7 ± 3.4 and 52.0 ± 5.4 nm for anterior and posterior stroma, respectively, $P > 0.99$ at both locations) and did not significantly differ between BSS and untreated controls. No difference in the diameter of the collagen fibers in HAse- or BSS-injected corneas was observed at any timepoint versus untreated controls ($P > 0.05$, Fig. 5C).

Discussion

The use of HAse for medical applications has dramatically increased in the past decade. Specifically, HAse has been used to enhance the penetration of local anesthetics in dermal and ophthalmic surgery[15,16] and has been reported to accelerate cutaneous wound healing in mice.[17] Despite its utility in the medical field, little is known about the impact of HAse on the biomechanics and structure of the tissues it is used in. In the present study, we quantitatively evaluated the enzymatic effects of HAse on the mechanical properties and ultrastructure of the cornea. The observation of increased corneal stromal stiffness following HAse injection in normal rabbit contrasts with a recent clinical study whereby injection of HAse reduced the stiffness of muscle tissue in patients with upper limb spasticity.[29] Muscle stiffness in spasticity is defined by resistance of muscle to passive movement and is a disorder in individuals affected by neurologic injury of cerebral and spinal origin.[29] Furthermore, our data also call into question the widely held belief that HAse softens tissues to reduce scarring and increases drug penetration.[15,16,30] These observations suggest that the function of HAse may be tissue and disease specific as well as dependent on the endogenous amount of HA and other GAG substrates expressed in the tissue. Further studies are warranted to determine the impact of HAse on the biomechanics and structure of normal and fibrotic dermal and muscle tissue.

We documented a reduction in collagen interfibrillar spacing concomitant with an increase in elastic modulus in HAse-treated corneas at days 1 and 7 postinjection consistent with a recent study that showed that crosslinking of chondroitin sulfate leads to denser collagen packing and an elevation of corneal stiffness.[31] Thus, the increase in elastic modulus is likely due to a decrease in viscoelastic behavior of the corneal stroma influenced by the packing of the collagen fibers. In aggregate, these data suggest that proteoglycans are critical to the intrinsic biomechanics of the cornea. Our laboratory has demonstrated that biophysical cues such as substratum topography and compliance profoundly influence keratocyte activation and their subsequent transformation into fibroblasts and myofibroblasts, a process known as keratocyte-fibroblast-myofibroblast (KFM) transformation.[32–35] We have also shown that maximal corneal stiffness following phototherapeutic

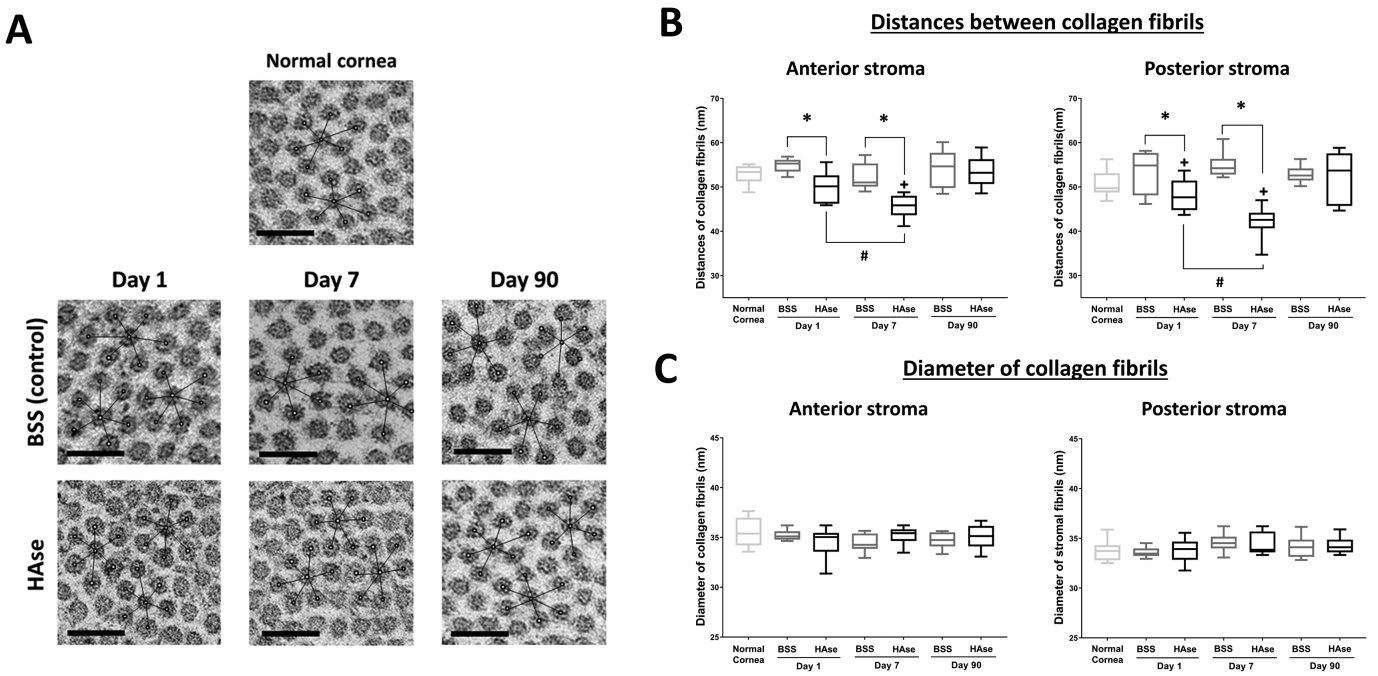

Figure 5. Intrastromal injection with HAse transiently decreased the interfibrillar spacing between the stromal collagens. (A) Increased packing of collagen fibrils was observed by TEM at days 1 and 7 in HAse-injected corneas versus BSS-treated and untreated controls; interfibrillar spacing returned to normal at day 90 in the HAse-treated group. (B) Quantitative analysis of the collagen spacing confirmed the aforementioned findings. (C) No change was observed in the diameter of the collagen fibrils throughout the study in all 3 groups. Results are expressed as mean ± SD. $^{+}P < 0.05$ compared to baseline, $^{*}P < 0.05$ in between days 1 and 7 in the same group, $^{\#}P < 0.05$ between the HAse- and BSS-treated groups at the same time point, 1-way ANOVA, followed by Tukey's pairwise multiple comparison test.

keratectomy in a rabbit model precedes stromal haze formation.[8,27] Wound healing involves a synchronized series of biophysical, cellular, and soluble cues participating in a coordinated fashion. While we did not observe a promotion of fibrosis when HAse was introduced after wounding, an adverse consequence on wound-healing outcomes cannot be ruled out if HAse had been administered prior to or concurrent with wounding.

The relationship between the AFM's applied force, indentation depth, and elastic modulus of the cornea has been validated by our group.[8,27] Using AFM, we determined that applying force of 1 nN indents the cornea up to the 200 nm in depth, which is significantly less than the thickness of the cornea measured in this study. Therefore, we exclude the effect of the substratum and also adhesives in our elastic modulus calculations. Despite transiently increasing collagen stiffness, intrastromal injection of HAse did not initiate the development of stromal haze in the normal cornea, although transient changes to keratocyte morphology observed with IVCM were observed. However, an organized arrangement of collagen fibrils is critical for corneal transparency.[10] Our results and others show that reduction in interfibrillar spacing does not promote corneal opacification as long as the decrease is uniform.[4,14] Acknowledged is the understanding that development as a relevant therapeutic to promote durable stiffening of the cornea would require novel approaches to maintain HAse activity long term either through linking the enzyme to stromal elements or integration with other approaches that maintain a durable presence with maintenance of activity. Corneal collagen crosslinking was introduced as a method to stiffen the cornea in diseases such as keratoconus to stabilize insidious malacic progression.[36] Adverse events associated with crosslinking such as anterior keratocyte apoptosis, infection, corneal edema, corneal nerve damage, and stromal haze have been reported.[37,38] In addition to these postoperative complications, separate studies have also shown that mutations in stromal proteoglycans can lead to random space reductions between adjacent collagen fibrils; formation of larger, more variable collagen fibrils; and corneal opacity.[39] The transformation of keratocytes to activated fibroblasts and myofibroblasts while critical to corneal wound healing is known to be a major contributing factor in the development of corneal haze and fibrosis.[40,41] Although a subtle change in keratocyte morphology was observed in the

first week following HAse injection, transformation to fibroblasts and myofibroblasts was not observed.[42] However, the use of HAse in fibrotic corneas may have markedly different results and warrants further study.

One study suggested that HAse may soften the corneal stroma possibly through altering its structure.[14] The enzymatic effect of HAse has also been investigated in combination with surgical procedures such as DALK.[24,25] These studies showed that HAse facilitated the separation of corneal stroma from DM in patients, possible through cleavage of chemical bonds between the stromal lamellae and/or between lamellae and DM. Following intrastromal injection of the HAse and BSS, in our present study, an immediate increase in central corneal thickness as well as corneal opacity at the injection site due to stromal edema was observed. These changes were due to temporary accumulation of the solutions injected into corneas, as demonstrated by FD-OCT and digital photography. A significant decrease in central corneal thickness was observed within 1 day following HAse injection in comparison to the untreated control group, which is consistent with previous studies.[14,25] The rate at which the HAse-injected corneas thinned directly correlated with the enzymatic activity of HAse in the corneal stroma as HAse has a direct destructive effect on GAG components such as HA and CS.[2–4] In cosmetics, the HAse half-life is determined to be around 2 minutes in HA-enriched conditions.[43] However, its effectiveness on the dermal tissues has been estimated to last for up to 48 hours despite its degradation.[44] Although we did not test the half-life of the HAse in our experiments, the prolonged effects of HAse seen in our experiments are unsurprising given that HA is not endogenously present in the rabbit's corneal stroma but is primarily synthesized following injury and during wound healing.[45] Interestingly, the rate at which HAse degrades CS is shown to be longer than that of HA.[46] Therefore, slow degradation of CS by HAse may be responsible for the gradual decrease of the central corneal thickness observed at day 7 postinjection. The interfibrillar spacing that is maintained (although reduced), observed at day 7 in the HAse-treated corneas, may be from the remaining KS, which is resistant to hydrolytic activity of HAse. Data on central thickness of the cornea corresponded well to ELISA measurements, which detected the presence of HAse activity in aqueous humor over time. We observed a relationship between the lower concentration of HAse in aqueous humor at day 7 and initiation of the corneal thickening beginning at the same time point, indicating a correlation between the washout rate of the HAse and gradual GAG repopulation in the corneal stroma. Given that the decrease in corneal thickness and the increase in stiffness were correlated, we would expect that the stiffness would return to baseline 4 to 6 weeks after injection. This suggests that monthly to bimonthly treatments may be necessary clinically. Further studies are required to determine how long the stiffening of the cornea lasts post-HAse injection for therapeutic purposes.

The only corneal opacity observed in the present study was mild infiltration of limbal vessels into the peripheral cornea in the HAse-injected corneas at days 14, 21, and 28. It has been shown that even purified animal-derived HAse extracts are usually contaminated with proteases, immunoglobulin, and other elements that can cause increased capillary permeability and hypersensitivity reactions.[47–50] Studies have also shown that HAse extracts are contaminated with large amounts of angiogenic growth factors.[51] Consideration of these contaminants is particularly critical when using HAse for introduction into the transparent avascular cornea. In addition, contamination with factors that promote neovascularization such as Vascular endothelial growth factor (VEGF) could predispose to development of pathologies in the eye such as neovascular glaucoma.[52] Impurities in HAse have also been implicated in cases of corneal endothelial toxicity.[53] However, in the present study, no changes to corneal endothelial morphology or density were observed using IVCM, histology, or TEM, likely due to the use of a chromatographically purified HAse, which demonstrates less corneal endothelial toxicity in comparison to HAse purified by other methods.[53] Thus, ophthalmologists using HAse for ocular applications should ensure that a chromatographically purified HAse is chosen.

In conclusion, degradation of GAG components by HAse gradually decreases the central corneal thickness through reduction of interfibrillar space. The increased packing of the collagen fibrils, concomitant with reduction of the proteoglycans, significantly increased the stiffness of the corneal stroma in a time-dependent manner but did not impact transparency of the treated corneas. Altering the mechanical properties of the corneal stroma has long been the target of various clinical procedures such as crosslinking and DALK. Here we show that HAse modulates the mechanical properties of the corneal stroma with minimal complications and suggests that it holds promise as a development target as an adjunctive corneal therapeutic.

Acknowledgments

Supported by the National Institutes of Health R01 EY019970 and P30 EY12576.

Disclosure: **S. Kim**, None; **I. Jalilian**, None; **S.M. Thomasy**, None; **M.A.W. Bowman**, None; **V.K. Raghunathan**, None; **Y. Song**, None; **C.A. Reinhart-King**, None; **C.J. Murphy**, None

* SK and IJ contributed equally to this work and should be considered as first authors.

† SMT and CJM should be considered co-corresponding authors.

References

1. Meek KM, Leonard DW. Ultrastructure of the corneal stroma: a comparative study. *Biophys J*. 1993;64:273–280.
2. Knepper PA, Farbman AI, Telser AG. Exogenous hyaluronidases and degradation of hyaluronic acid in the rabbit eye. *Invest Ophthalmol Vis Sci*. 1984;25:286–293.
3. Honda T, Kaneiwa T, Mizumoto S, Sugahara K, Yamada S. Hyaluronidases have strong hydrolytic activity toward chondroitin 4-sulfate comparable to that for hyaluronan. *Biomolecules*. 2012;2:549–563.
4. Knudson W, Gundlach MW, Schmid TM, Conrad HE. Selective hydrolysis of chondroitin sulfates by hyaluronidase. *Biochemistry (Mosc)*. 1984;23:368–375.
5. Scott JE. Proteoglycan collagen interactions and corneal ultrastructure. *Biochem Soc Trans*. 1991;19:877–881.
6. Meek KM, Elliott GF, Nave C. A synchroton x-ray diffraction study of bovine cornea stained with cupromeronic blue. *Coll Res Rel*. 1986;6:203–218.
7. Scott JE, Haigh M. 'Small'-proteoglycan: collagen interactions:keratan sulphate proteoglycan associates with rabbit corneal collagen fibrils at the 'a' and 'c' bands. *Biosci Rep*. 1985;4:765–774.
8. Raghunathan VK, Thomasy SM, StrØm P, Yañez-Soto B, Garland SP, Sermeno J, Reilly CM, Murphy CJ. Tissue and cellular biomechanics during corneal wound injury and repair. *Acta Biomaterialia*. 2017;58:291–301.
9. Myrna KE, Mendonsa R, Russell P, Pot SA, Liliensiek SJ, Jester JV, Nealey PF, Brown D, Murphy CJ. Substratum topography modulates corneal fibroblast to myofibroblast transformation. *Invest Ophthalmol Vis Sci*. 2012:53:811–816.
10. Maurice DM. The structure and transparency of the cornea. *J Physiol*. 1957;136:263–286.
11. Jester JV, Barry-Lane PA, Cavanagh HD, Petroll WM. Induction of α-smooth muscle actin expression and myofibroblast transformation in cultured corneal keratocytes. *Cornea*. 1996;15:505–516.
12. Dreier B, Thomasy SM, Mendonsa R, Raghunathan VK, Russell P, Murphy CJ. Substratum compliance modulates corneal fibroblast to myofibroblast transformation. *Invest Ophthalmol Vis Sci*. 2013;54:5901–5907.
13. Frost GI. Recombinant human hyaluronidase (rHuPH20): an enabling platform for subcutaneous drug and fluid administration. *Expert Opin Drug Deliv*. 2007;4:427–440.
14. Connon CJ, Meek KM, Newton RH, Kenney MC, Alba SA, Karageozian H. Hyaluronidase treatment, collagen fibril packing, and normal transparency in rabbit corneas. *J Refract Surg*. 2000;16:448–455.
15. Wohlrab J, Finke R, Franke WG, Wohlrab A. Clinical trial for safety evaluation of hyaluronidase as diffusion enhancing adjuvant for infiltration analgesia of skin with lidocaine. *Dermatol Surg*. 2012;38:91–96.
16. Moharib MM, Mitra S. Alkalinized lidocaine and bupivacaine with hyaluronidase for subtenon's ophthalmic block. *Reg Anesth Pain Med*. 2000;25:514–517.
17. Fronza M, Caetano GF, Leite MN, Bitencourt CS, Paula-Silva FWG, Andrade TAM. Hyaluronidase modulates inflammatory response and accelerates the cutaneous wound healing. *PLoS ONE*. 2014;9:e112297.
18. Pirie A. The effect of hyaluronidase injection on the vitreous humour of the rabbit. *Br J Ophthalmol*. 1949;33:678–684.
19. Harooni M, McMillan T, Refojo M. Efficacy and safety of enzymatic posterior vitreous detachment by intravitreal injection of hyaluronidase (see comments). *Retina*. 1998;18:16–22.
20. Gum GG, Samuelson DA, Gelatt KN. Effect of hyaluronidase on aqueous outflow resistance in normotensive and glaucomatous eyes of dogs. *Am J Vet Res*. 1992;53:767–770.
21. Kupperman BD, Thomas EL, Graue F, de la Fuente MA, Quiroz-Mercado H, Guerrero JL, Giamporcaro JE, Giulle SL, Reyes E, Shibuya R. Clearance of vitreous hemorrhage after intravitreal administration of hyaluronidase pre-clinical pharmacology and clinical outcomes (ARVO Abst. No. 1814). *Invest Ophthalmol Vis Sci*. 2000;41:B60.
22. Harooni M, Freilich JM, Abelson M, Refojo M. Efficacy of hyaluronidase in reducing increases in intraocular pressure related to the use of viscoelastic substances. *Arch Ophthalmol*. 1998;116:1218–1221.

23. Lambert RW, Wagstaff RE, Vu C, Karageozian HL, Rich KA. Resolution of human corneal scars by ACS-hyaluronidase (ARVO Abst. No. 3704). *Invest Ophthalmol Vis Sci*. 2000;41: B802.
24. Bonci P, Bonci P, Della Valle V, Fanini F, Nardi-Pantoli A. Enzymatic descemetic lamellar keratoplasty: pilot study. *Eur J Ophthalmol*. 2010;20:879–884.
25. Lange AP, Moloney G, Arino M, Ng A, McCarthy JM, White VA, Holland SP. Enzyme-assisted deep anterior lamellar keratoplasty—a new method of lamellar dissection—a wetlab-based pilot study. *Cornea*. 2013;32:98–103.
26. Eaton JS, Miller PE, Bentley E, Thomasy SM, Murphy CJ. The SPOTS system: an ocular scoring system optimized for use in modern preclinical drug development and toxicology. *J Ocul Pharmacol Ther*. 2017;33:718–734.
27. Thomasy SM, Raghunathan VK, Winkler M, Reilly CM, Sadeli AR, Russell P, Jester JV, Murphy CJ. Elastic modulus and collagen organization of the rabbit cornea: epithelium to endothelium. *Acta Biomater*. 2014;10:785e791.
28. Maggs D, Miller P, Ofri R. *Slatter's Fundamentals of Veterinary Ophthalmology*. 5th ed. Philadelphia, PA: Saunders; 2012.
29. Raghavan P, Lu Y, Mirchandani M, Stecco A. Human recombinant hyaluronidase injections for upper limb muscle stiffness in individuals with cerebral injury: a case series. *EBioMedicine*. 2016;9:306–313.
30. Cornbleet T. Treatment of keloids with hyaluronidase. *J Am Med Assoc*. 1954:154:1161–1163.
31. Wang X, Majumdar S, Ma G, Sohn J, Yiu SC, Stark W, Al-Qarni A, Edward DP, Elisseeff JH. Chondroitin sulfate-based biocompatible crosslinker restores corneal mechanics and collagen alignment. *Invest Ophthalmol Vis Sci*. 2017;58:3887–3895.
32. Myrna KE, Pot SA, Murphy CJ. Meet the corneal myofibroblast: the role of myofibroblast transformation in corneal wound healing and pathology, *Vet Ophthalmol*. 2009;12:25–27.
33. Snyder MC, Bergmanson JP, Doughty MJ. Keratocytes: no more the quiet cells. *J Am Optom Assoc*. 1998;69:180–187.
34. Jester JV, Petroll WM, Barry PA, Cavanagh HD. Expression of α-smooth muscle (α-SM) actin during corneal stromal wound healing. *Invest Ophthalmol Vis Sci*. 1995;36:809–819.
35. Netto MV, Mohan RR, Ambrosio R, Jr, Hutcheon AE, Zieske JD, Wilson SE. Wound healing in the cornea: a review of refractive surgery complications and new prospects for therapy. *Cornea*. 2005;24:509–522.
36. Wollensak G, Spoerl E, Seiler T. Riboflavin/ultraviolet-A-induced collagen crosslinking for the treatment of keratoconus. *Am J Ophthalmol*. 2003;135:620–627.
37. Evangelista CB, Hatch KM. Corneal collagen cross-linking complications. *Semin Ophthalmol*. 2018;33:29–35.
38. Salomao MQ, Chaurasia SS, Sinha-Roy A, Ambrosio R, Jr, Esposito A, Sepulveda R, Agrawal V, Wilson SE. Corneal wound healing after ultraviolet-A/riboflavin collagen cross-linking: a rabbit study. *J Refract Surg*. 2011;27:401–407.
39. Chakravarti S, Magnuson T, Lass JH, Jepsen KJ, LaMantia C, Carroll H. Lumican regulates collagen fibril assembly: skin fragility and corneal opacity in the absence of lumican. *J Cell Biol*. 1998;141:1277–1286.
40. Torricelli AA, Wilson SE. Cellular and extracellular matrix modulation of corneal stromal opacity. *Exp Eye Res*. 2014;129: 151–160.
41. Jester JV, Moller-Pedersen T, Huang J, Sax CM, Kays WT, Cavangh HD, Petroll WM, Piatigorsky J. The cellular basis of corneal transparency: evidence for 'corneal crystallins'. *J Cell Sci*. 1999;112(Pt 5):613–622.
42. Jester JV, Petroll WM, Barry PA, Cavanagh HD. Temporal, 3-dimensional, cellular anatomy of corneal wound tissue. *J Anat*. 1995;186(Pt 2):301–311.
43. Quezada-Gaón N, Wortsman X. Ultrasound-guided hyaluronidase injection in cosmetic complications. *J Eur Acad Dermatol Venereol*. 2016;30:e39–e40.
44. Bailey SH, Fagien S, Rohrich RJ. Changing role of hyaluronidase in plastic surgery. *Plast Reconstr Surg*. 2014;133:127e–132e.
45. Krachmer JH, Mannis MJ, Holland EJ. *Cornea*. 3rd ed. St. Louis, MO: Mosby; 2011.
46. Stern R, Jedrzejas MJ. Hyaluronidases: their genomics, structures, and mechanisms of action. *Chem Rev*. 2006;106:818–839.
47. Benditt EP, Schiller S, Mathews MB, Dorfman A. Evidence that hyaluronidase is not the factor in testicular extract causing increased vascular permeability. *Proc Soc Exp Biol Med*. 1951;77: 643–645.
48. Kind LS, Roffler S. Adverse reactions to hyaluronidase. *Proc Soc Exp Biol Med*. 1961;106:734–735.

49. Schwartzman J. Hyaluronidase in pediatrics. *NY State J Med*. 1951;51:215–221.
50. Silverstein SM, Greenbaum S, Stern R. Hyaluronidase in ophthalmology. *J Appl Res*. 2012;12:1–13.
51. Rahmanian M, Heldin P. Testicular hyaluronidase induces tubular structures of endothelial cells grown in three-dimensional collagen gel through a CD44-mediated mechanism. *Int J Cancer*. 2002;97:601–607.
52. Tripathi RC, Lixa J, Tripathi BJ, Chalam KV, Adamis AP. Increased level of vascular endothelial growth factor in aqueous humor of patients with neovascular glaucoma. *Ophthalmology*. 1998;105:232–237.
53. Jumper JM, McCauley MB, Equi RA, Duncan KG, Duncan J, Schwartz DM. Corneal toxicity of intraocular hyaluronidase. *J Ocul Pharmacol Ther*. 2002;18:89–97.